

Fig. 1.3: Different contributions to the energy resolution of the PbWO_4 calorimeter.

Angular and mass resolution

The two-photon mass resolution depends on the energy resolution and the error on the measured angle between the two photons. If the vertex position is known, the angular error is negligible. However, a contribution of about 1.5 GeV to the di-photon mass resolution (at a mass of around 100 GeV) is expected from the uncertainty in the position of the interaction vertex, if the only information available is the r.m.s spread of about 5.3 cm of the interaction vertices. At low luminosity, where the number of superimposed events is small, the longitudinal position of the Higgs production vertex can be localized using high- p_T tracks originating from the Higgs event. Studies indicate that even at high luminosity the correct vertex can be located for a large fraction of events using charged tracks. However, this result depends on the precise knowledge of the minimum-bias pileup at LHC energies. We thus retain the possibility of inserting a barrel preshower device consisting of a lead/silicon layer. The information from the preshower, when combined with that of the crystal calorimeter, could provide the measurement of the photon direction at high luminosity, with an accuracy of about $45 \text{ mrad}/\sqrt{E}$.

1.4.4 Radiation environment

At a luminosity of $10^{34} \text{ cm}^{-2} \text{ s}^{-1}$ about 10^9 inelastic proton-proton interactions per second will generate a hostile radiation environment.

The simulations of the radiation environment use minimum-bias events obtained from the DPMJET-II event generator. The uncertainty in the estimate of the neutron fluence is about a factor of 2 due to approximations in the geometrical descriptions of the subdetectors, and somewhat smaller for the dose in and around the ECAL. All estimates are presented for an integrated luminosity of $5 \times 10^5 \text{ pb}^{-1}$ assumed to be appropriate for the first ten years of LHC operation.

The dose

The integrated dose at the shower maximum in the crystals and around the crystals at various values of the pseudorapidity is given in Fig. 1.4. The integrated dose at shower maximum in the barrel crystals is about 4 kGy whereas it rises to about 90 kGy and 200 kGy at $|\eta| = 2.6$ and $|\eta| = 3$ respectively.

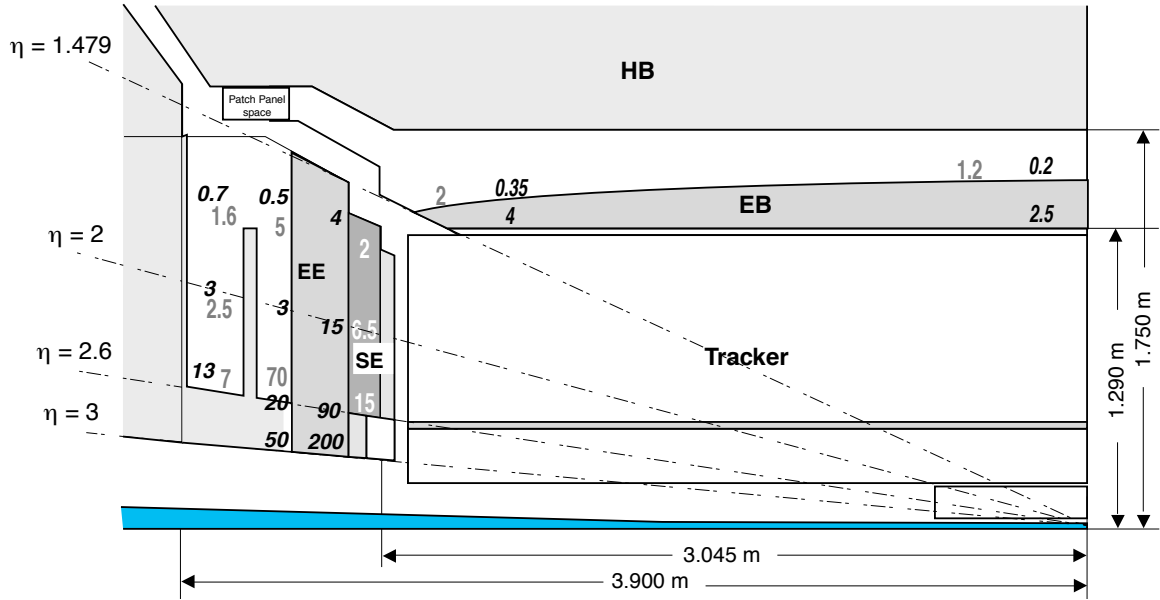


Fig. 1.4: The dose and neutron fluence in and around the crystals as a function of pseudorapidity. Numbers in bold italics are doses, in kGy, at shower maximum and at the rear of the crystals. The other numbers are fluences immediately behind the crystals, in the space for endcap electronics surrounded by moderators and in the silicon of the preshower in units of 10^{13} cm^{-2} . All values correspond to an integrated luminosity of $5 \times 10^5 \text{ pb}^{-1}$ appropriate for the first ten years of LHC operation.

The neutron fluence

Hadron cascades in the crystals lead to a large neutron albedo emerging from the ECAL. The fluence of neutrons with energies above 100 keV is shown in Fig. 1.4 for various values of pseudorapidity. Knowledge of the neutron fluence behind the barrel part of the ECAL is important for estimating the increase in APD leakage currents due to radiation damage.

Because of the large neutron fluence in the endcap, VPTs have been chosen for this region. The front-end electronics are separated from the VPTs and located in a space surrounded by polyethylene moderators. The neutron fluence and absorbed dose in this region, at a radius as low as 60 cm, are below $7 \times 10^{13} \text{ n cm}^{-2}$ and 13 kGy respectively.

With an optimized design of moderators, the neutron fluence at the location of Si detectors of the endcap and barrel preshowers can be kept below $15 \times 10^{13} \text{ n cm}^{-2}$ and $2 \times 10^{13} \text{ n cm}^{-2}$ respectively.

- stabilize the temperature of the calorimeter to ≤ 0.1 °C.

A 3-D view of the barrel and endcap electromagnetic calorimeter is shown in Fig. 1.5.

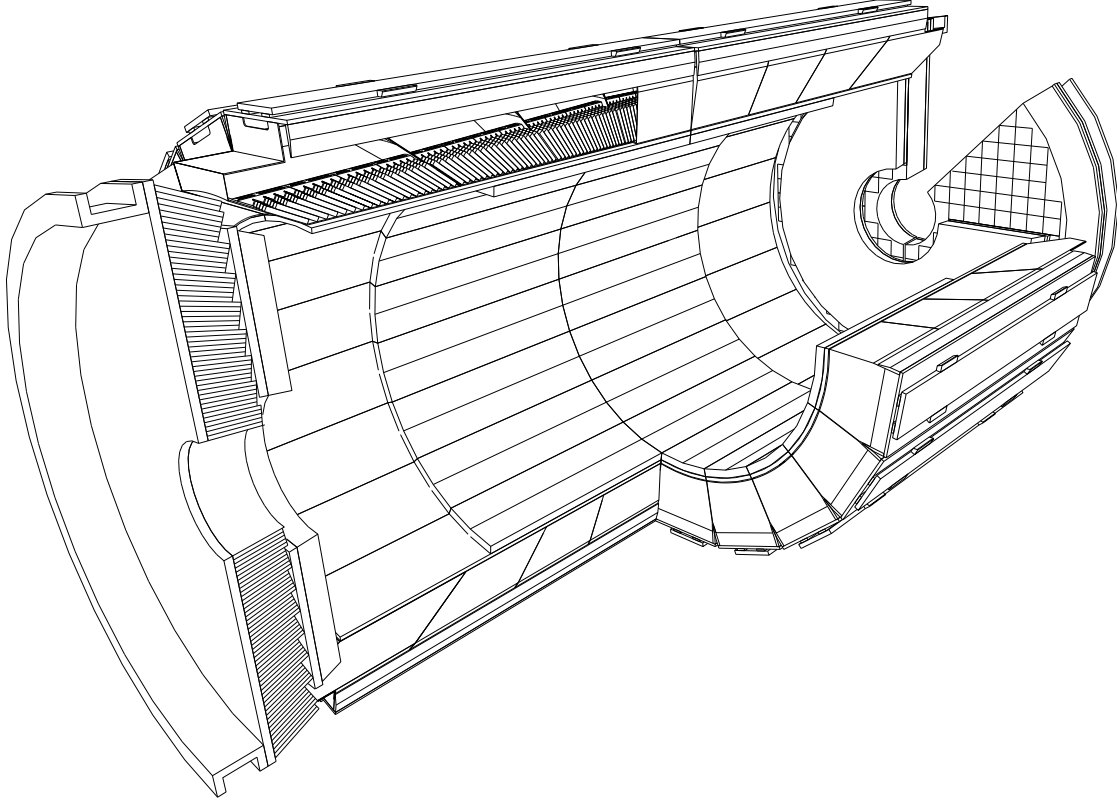


Fig. 1.5: A 3-D view of the electromagnetic calorimeter.

1.6.1 The barrel calorimeter

The barrel part of the ECAL covers the pseudorapidity range $|\eta| < 1.479$ (see Fig. 1.6). The front face of the crystals is at a radius of 1.29 m and each crystal has a square cross-section of $\approx 22 \times 22$ mm² and a length of 230 mm corresponding to $25.8 X_0$. The truncated pyramid-shaped crystals are mounted in a geometry which is off-pointing with respect to the mean position of the primary interaction vertex, with a 3° tilt in both ϕ and in η . The crystal cross-section corresponds to $\Delta\eta \times \Delta\phi = 0.0175 \times 0.0175$ (1°). The barrel granularity is 360-fold in ϕ and (2×85) -fold in η , resulting in a total number of 61 200 crystals. The crystal volume in the barrel amounts to 8.14 m³ (67.4 t). Crystals for each half-barrel will be grouped in 18 supermodules each subtending 20° in ϕ . Each supermodule will comprise four modules with 500 crystals in the first module and 400 crystals in each of the remaining three modules. For simplicity of construction and assembly, crystals have been grouped in arrays of 2×5 crystals which are contained in a very thin wall (200 μ m) alveolar structure and form a submodule.

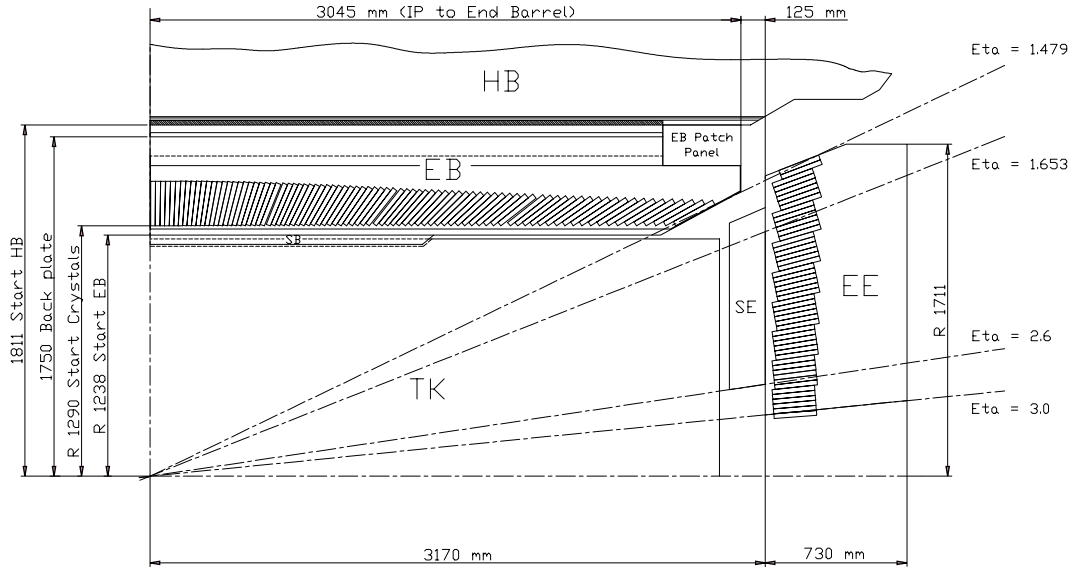


Fig. 1.6: Longitudinal section of the electromagnetic calorimeter (one quadrant).

Table 1.2 summarizes the design parameters. Figure 1.7 displays the total thickness (in radiation lengths) of the ECAL as a function of pseudorapidity. The crystal-to-crystal separation across intermodule boundaries is 6 mm (both in η and ϕ), and results in the radiation lengths reduction shown in Fig. 1.7.

Table 1.2: ECAL design parameters

Parameter	Barrel	Endcaps
Pseudorapidity coverage	$ \eta < 1.48$	$1.48 < \eta < 3.0$
ECAL envelope: $r_{\text{inner}}, r_{\text{outer}}$ [mm]	1238, 1750	316, 1711
ECAL envelope: $z_{\text{inner}}, z_{\text{outer}}$ [mm]	0, ± 3045	$\pm 3170, \pm 3900$
Granularity: $\Delta\eta \times \Delta\phi$	0.0175×0.0175	0.0175×0.0175 to 0.05×0.05
Crystal dimension [mm ³]	typical: $21.8 \times 21.8 \times 230$	$24.7 \times 24.7 \times 220$
Depth in X_0	25.8	24.7
No. of crystals	61 200	21 528
Total crystal volume [m ³]	8.14	3.04
Total crystal weight [t]	67.4	25.2
Modularity	36 supermodules	4 Dees
1 supermodule/Dee	1700 crystals (20 in ϕ , 85 in η)	5382 crystals
1 supercrystal unit	–	36 crystals

Thermal regulation will be carried out by two active systems: (i) a specially regulated cooling circuit which keeps the operating temperature (ambient temperature) of the crystal array and of the APDs within a tight temperature spread of ± 0.05 °C, ensuring adequate thermal stability; (ii) the power cooling circuit evacuates the heat generated by all power sources in the supermodule (each supermodule is designed as a separate thermal entity).

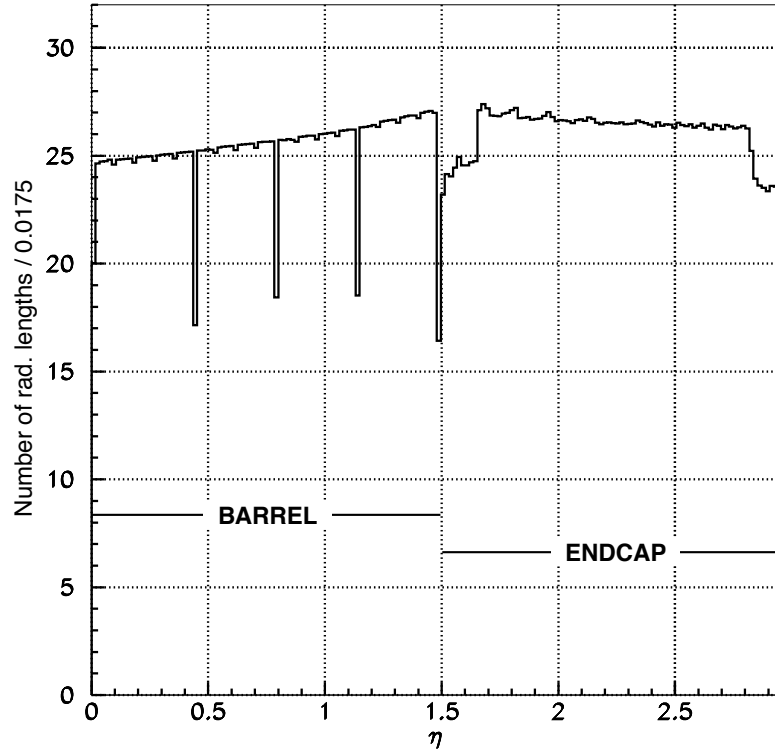


Fig. 1.7: Total thickness in X_0 of the ECAL as a function of pseudorapidity, averaged over ϕ .

1.6.2 The endcap calorimeter

The endcap part of the crystal calorimeter covers a pseudorapidity range from 1.48 to 3.0. The design of the endcaps provides precision energy measurement to $|\eta| = 2.6$. Crystals will however be installed up to $|\eta| = 3$ in order to augment the energy-flow measurement in the forward direction.

The mechanical design of the endcap calorimeter is based on an off-pointing pseudo-projective geometry using tapered crystals of the same shape and dimensions ($24.7 \times 24.7 \times 220 \text{ mm}^3$) grouped together into units of 36, referred to as supercrystals. A total of 268 identical supercrystals will be used to cover each endcap with a further 64 sectioned supercrystals used to complete the inner and outer perimeter. Each endcap contains 10 764 crystals, corresponding to a volume of 1.52 m^3 (12.6 t). Both endcaps are identical. Each endcap detector is constructed using Dee-shaped sections as seen in Fig. 1.8. Table 1.2 summarizes the design parameters.

Figure 1.7 shows the total thickness (in radiation lengths) of the ECAL as a function of pseudorapidity; where the endcap part also includes the preshower detector.

Because of the high radiation levels in the endcaps (see Fig. 1.4) all materials used in this region must tolerate very large doses and neutron fluences.

The endcap calorimeter will be operated at a temperature close to ambient, which must be stabilized to within $0.1 \text{ }^\circ\text{C}$. The preshower detector mounted in front of the endcaps will be operated at $-5 \text{ }^\circ\text{C}$, thus care must be taken to avoid any condensation problems. Cooling

requirements for individual crystals will be met by means of the thermal conduit provided from the rear face of the crystal through the metal inserts to the interface plate and support elements. Cooling regulation will be provided by a water cooling system installed on the Dee support plate.

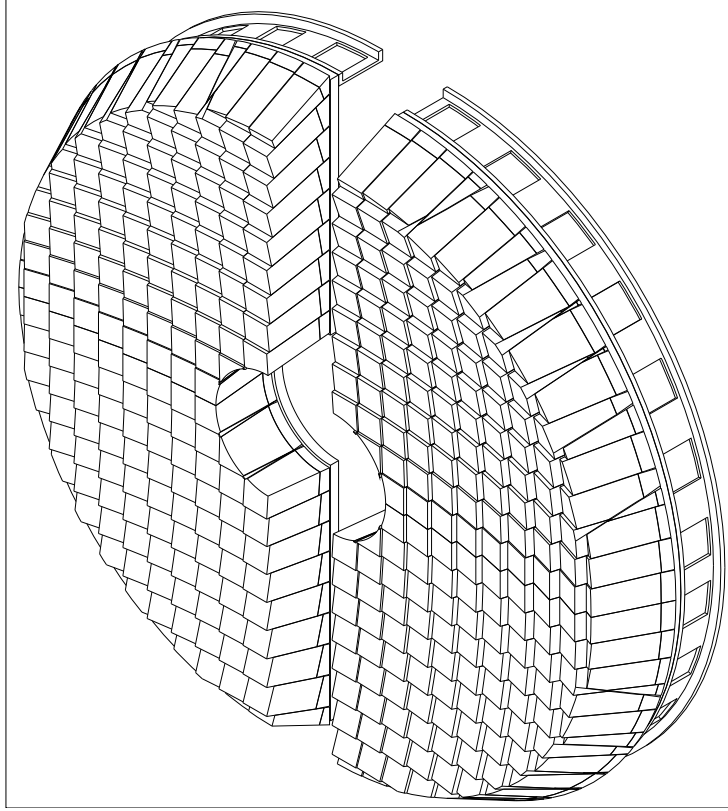


Fig. 1.8: A single endcap with Dees apart.

1.6.3 The preshower detectors

The endcap preshower covers a pseudorapidity range from $|\eta| = 1.65$ to 2.61 . It will be present from the start of the experiment. Its main function is to provide π^0 - γ separation. In the barrel, an optional preshower covers the pseudorapidity range up to $|\eta| = 0.9$ to enable measurement of the photon angle to an accuracy of about $45 \text{ mrad}/\sqrt{E}$ in the η direction. This detector will be built and installed only for the high-luminosity operation, if the activity of the minimum-bias events seen at LHC start-up shows that additional angular determination is necessary.

The preshower detector, placed in front of the crystals, contains lead converters (a single one of $2.5 X_0$ in the barrel, two converters in the endcaps of a total thickness of $2 X_0$ and $1 X_0$ respectively), followed by detector planes of silicon strips with a pitch of $< 2 \text{ mm}$. The impact position of the electromagnetic shower is determined by the centre-of-gravity of the deposited energy. The accuracy is typically $300 \text{ }\mu\text{m}$ at 50 GeV . In order to correct for the energy deposited in the lead converter, the energy measured in the silicon is used to apply corrections to the energy measurement in the crystal. The fraction of energy deposited in the preshower (typically 5% at 20 GeV) decreases with increasing incident energy. Figure 1.9 shows the layout of the preshower, and Table 1.3 summarizes the design parameters.

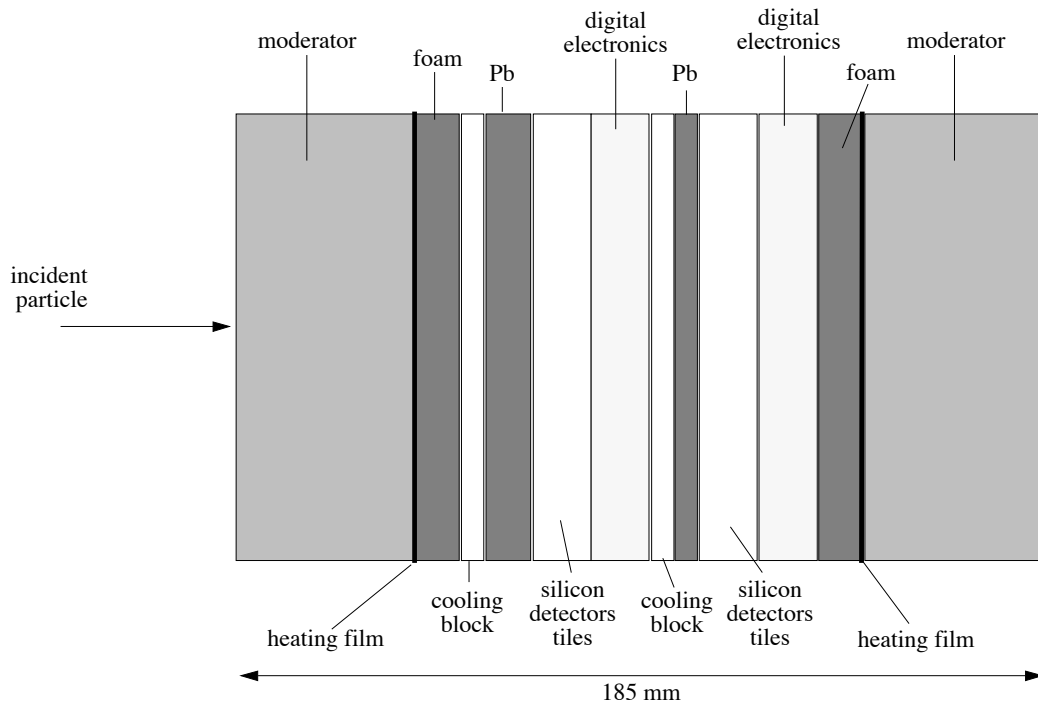


Fig. 1.9: Schematic section through the endcap preshower.

Table 1.3: Preshower design parameters

	Barrel	Endcap
$ \eta $ – range	0–0.9	1.65–2.61
Fiducial area	17.8 m ²	16.4 m ²
Si detectors	2880 × 2	4512
Strip pitch / length	1.8 mm / 102 mm	1.9 mm / 61 mm
Electronics channels	92 160	144 384
Operating temperature	12 °C	–5 °C
Max. integrated fluence	1.25×10^{13} n/cm ²	1.6×10^{14} n/cm ²
Max. integrated dose	~ 5 kGy	~ 70 kGy

To maintain its performance during the lifetime of the experiment, the endcap silicon detector has to be operated at –5 °C. Heating films and insulating foam glued on the moderators guarantee that the external surfaces are kept at the ambient temperature of the neighbouring detectors.